Target recognition in synthetic aperture sonar and high resolution side scan sonar using AUVs

TARGET RECOGNITION IN SYNTHETIC APERTURE AND HIGH RESOLUTION SIDE-SCAN SONAR

Y. Petillot, Y. Pailhas, J. Sawas, N. Valeyrie, J. Bell

Oceans Systems Research Group, School of Engineering and Physical Sciences, Heriot-Watt University, Edinburgh, EH14 4AS (Y.R.Petillot@hw.ac.uk, Tel: 0131 451 8277, Fax: 0131 451 4155)

Abstract

The accurate detection and identification of underwater targets continues as a major issue, despite, or perhaps as a result of, the promise of higher resolution underwater imaging systems, including synthetic aperture sonar, high frequency sidescan and high resolution cameras. Numerous techniques have been proposed for Computer Aided Detection to detect all possible mine-like objects, and Computer Aided Classification to classify whether the detected object is a target or not. The majority of existing techniques have concentrated on the analysis of the acoustic shadow casted by the objects. With the development of ultra high-resolution systems, new techniques inherited from the computer vision community can now be applied, taking into account the acoustic echo and shadow. This paper will briefly review traditional techniques and present new possible solutions to the problem of detection and classification in synthetic aperture sonar.

1 Target Detection and Classification

With the recent advances in autonomous underwater vehicle (AUV) technology for mine-countermeasures (MCM) the need has arisen for on-board automated techniques for object identification from sonar data. Research carried out in developing MCM tools is generally split into Computer Aided Detection (CAD)[1-4] to detect all possible mine-like objects, and Computer Aided Classification (CAC) models [6-11] to classify whether the detected object is a mine or not. A common approach is to compare a set of extracted features from the mine-like object (MLO) [6,3] to a set of pre-determined training data. The system is trained using a set of ground-truthed data before being run on the unknown "test" data. These approaches require a large amount of training data often unavailable as real experiments are very expensive and are often limited in scale. This can lead to over-fitting of the data when small datasets are used and limits the generalisation capabilities of such approaches [3]. Fusing the results from multiple classifiers using different feature sets and classification techniques can improve performance [11]. In general, these systems offer a black-box solution to the problem, and it can be difficult to analyse why a particular result is obtained.

Obtaining information other than the basic mine or not-mine label is usually referred to as object identification. Information such as the shape and dimension of the mine can allow the mine type to be determined and can help detail how best to neutralise the threat. Man-made objects such as mines generally have regular shapes and so leave regular shaped shadows in sidescan images. The shape of these shadows can be used to identify the objects by extracting relevant features from the shadows and comparing these to known training data [8]. The non-linear nature of the shadow-formation process ensures a shadow normalisation step is required for these approaches to be widely applicable.

This paper will briefly discuss and compare two possible solutions to this problem of trained systems. The first is a model based technique which uses a three stage process to detect and classify the targets, but which requires no training. The second solution is to employ simulation and augmented reality simulators to permit the generation of training data. This in turn enables the simulation of targets within real sonar data, allowing the training data to be tailored to the specific sonar system or the operating environment. With large amount of training data available and the improvement in resolution gained from synthetic aperture or very high frequency imaging (acoutics cameras), modern computer vision techniques can be used for detection and classification. This will be briefly demonstrated for each scenario.

2. High Resolution Imaging

Typical sidescan systems used for mine countermeasures applications can provide a resolution of between 3cm and 10cm depending on operating range and frequency. New very high frequency systems, such as the Marine-Sonics 2.4MHz system offers resolution of 1cm but is limited to operating ranges of less than 6m. Although such systems offer increased potential for improved classification, their use for detection of targets is limited as a result of their limited range.

The first commercially produced Synthetic Aperture Sonar (SAS) systems are now available, bringing the promise of higher resolution surveys at long ranges. In the area of Mine Countermeasures this offers the capability to detect mines at longer ranges and provide higher resolution images of targets for subsequent classification. However, little work has been done to investigate the automatic detection and classification of mines from SAS imagery, since previous research in this area concentrated on developing the sensor rather than the automated processing of the images, since it was always assumed that their higher resolution would simplify this task. However although providing higher resolution, the images contain a significant level of speckle due to the construction of the image. Filtering methods have been employed, but these can degrade either the shadow or the highlight. The shadow can also be altered by the SAS processing limiting the applicability of well established detection techniques in side-scan imagery.

3 Overview of Model Based Systems

Model based systems use strong prior information of the image formation process to guide the detection or identification of a target. We present here a model based system tailored for side-scan sonar imagery with potential applications to SAS data.

The model based technique [4,10] for the detection and classification of mine-like objects (MLOs) presented here has been developed to overcome the problems of trained systems with a three-stage process which is summarised in figure 1. The first stage is the detection of mine like objects (MLOs) within the sidescan sonar image. This stage uses a Markov Random Field (MRF) model to directly segment the image into regions of object highlight, shadow and background [4]. Unlike many previous models for object detection this requires no training. The structure of the MRF model also integrates specific priors that take into account the characteristics of sidescan data. Simple information such as the fact that a target is generally displayed as an area of object highlight followed by shadow, and that the highlight tends to form small clusters surrounded by background pixels can readily be integrated.

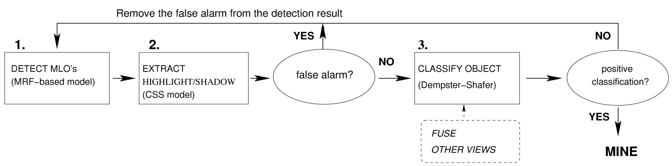

Figure 1: Overview of Detection and Classification System

The detected targets from this first stage are then passed to stage two, where the highlight and shadow regions of the detected objects are extracted using a Cooperating Statistical Snake technique (CSS)[4]. The CSS model approximates the background as three homogenous regions – object highlight, background and shadow and so uses two statistical snakes, one to segment the highlight and one the shadow. The a priori information between the highlight and shadow is used to constrain the movement of the snakes so as to achieve accurate segmentation results regardless of the seabed type involved.

The CSS model can also be used to eliminate false alarms from the detection stage. Areas can be indicated as object highlight and false alarms produced, especially from more complex regions such as sand ripples. If the CSS model is applied to these regions, since they do not have the expected characteristics of MLOs, the shadow snake will expand in an uncontrolled manner. If the snakes expand beyond mine-like dimensions the detection can be identified as a false alarm and removed.

After a detected MLO has passed through both the Detection and CSS modules, stage 3 of the system will classify the object. To do this, the system has the extracted shadow and object-highlight region of the MLO, as well as some simple information extracted from the navigation data, such as height of the sonar above the seabed and the range to the object at the time of ensonification. Although the highlight is generally not considered for classification purposes since it is generally unpredictable and difficult to model, basic information can be extracted from it and used together with the information from the shadow region.

The model represents possible mine-like shapes (cylinder, sphere, truncated-cone) using parametric models which allow a sonar simulator to generate the resulting shadow region from such an object. Each shadow region is specific to the particular parameters of each shape and is generated under the same sonar conditions as the MLO was detected. As the model searches through the different parameter options, the resulting synthetic shadows are compared to the real MLO shadow to find the best match for each considered class. This section of the model is the most computationally intensive and a detailed overview of this section is shown in Figure 2.

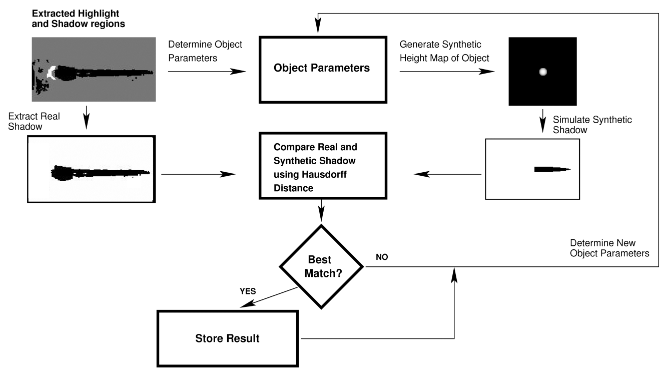

Figure 2: Determination of best synthetic shadow match to real shadow

Once this has been completed, the degree of match and the shape parameters used to obtain it are output to the classifier to define a class membership function. These membership functions are entered into a classifier which identifies the belief that the object belongs to a particular class.

As indicated in figure 1, the classification can also be extended to include multiple views [10] if the target has been seen from multiple angles.

3.1 Results with Sidescan

Table 1 illustrates the output of the classification system for 4 example sidescan images extracted from Edgetech DF1000 and Klein 5500 sonar data. This illustrates the successful classification of these targets.

Sidescan Images	**Belief**			
	Bel(cyl)	Bel(sph)	Bel(con)	Bel(clut)

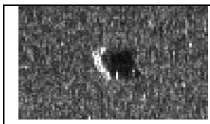 Cylinder	0.71	0	0	0.2
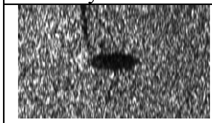 Sphere	0	0.833	0	0.083
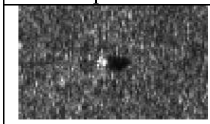 Cone	0	0.303	0.45	0.045
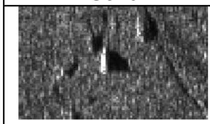 Clutter	0.42	0	0	0.46

3.2 SAS Results

The first two stages of the classification have been tested using SAS data from both a rail based system and an AUV. This used directly the software developed for processing the sidescan imagery with no modifications. The third stage which then undertakes the model-based classification could not be tested since this requires knowledge of the exact resolution of the images and slant ranges to targets to enable dimensions in metres to be extracted from the data.

The first step was the MRF based detection and results are illustrated in figure 3. In this case, both of the targets highlights were clearly identified and the shadow region of each target is apparent. However, the shadow region was not detected as “pure” shadow and contained regions labelled as seabed reverberation within the general shadow zone of the target. This was particularly apparent for the cylindrical target.

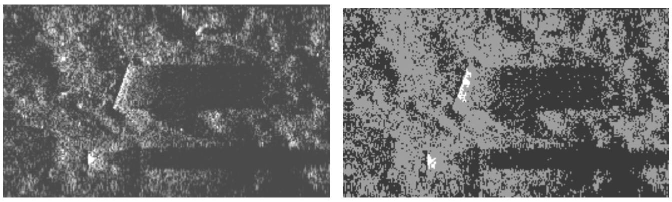

Figure 3: (a) SAS image of cylindrical and spherical target (b) MRF detection result (white represents target, black shadow and grey background reverberation)

However, the 2nd stage of the process, where the contours of the highlight and shadow are extracted using the CSS performed well. This technique is searching for areas with similar statistical properties and uses the original image and not the segmented image. The detection result is used purely to identify possible target regions, which are then to be examined for classification. The CSS has successfully been able to extract the contours of the shadow and the increased speckle within the shadow has not degraded the result.

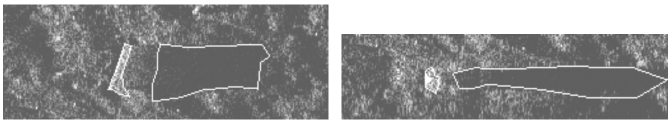

Figure 4: Extracted highlight and shadow regions using CSS (a) cylindrical target and (b) spherical target from figure 3

Results are also shown in figure 5 for a more complex cylindrical shape. The same characteristics were also noted, that the detection stage was able to successfully detect target regions containing the characteristic highlight and shadow, but that parts of the shadow region were often incorrectly labelled as seabed reverberation. The CSS was however able to successfully extract the contours of the highlight and the shadow, even although the detection model only labelled the bright bands on the target as highlight, the CSS was able to extract the entire region of target and not just the brightest reflectors on it.

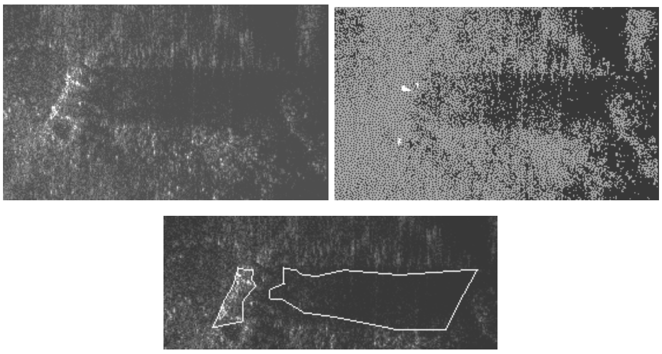

Figure 5: (a) SAS image of cylindrical target (b) MRF detection result (c) extracted highlight and shadow

Although it was only possible at this stage to assess the results of the first two stages of the process, the results appear promising, in that accurate contours of the objects highlight and shadow could be extracted in the majority of the cases and that this suggest no reason for the overall process not to be successful.

The SAS images are significantly higher resolution than the sidescan images which have previously been processed using this technique. In the majority of sidescan images the target highlight and shadow is typically only a few pixels. In these images much greater resolution was available. However, there was significant speckle present within the images.

The MRF detection-orientated segmentation requires no training, and estimates the Markovian parameters from the image. It does however assume that the likelihood term for the shadow class is Gaussian and the likelihood term for the seabed reverberation is a shifted Rayleigh [4]. Although, these assumptions are generally regarded as appropriate for sidescan imagery, the increased speckle of the SAS images may mean that these are no longer the most appropriate choices. In the results it can be noted that although the highlight is detected, it is sometimes only the brightest features within the overall highlight region. The shadow region is also detected not as a complete shadow, but with regions of seabed reverberation within it. This is probably due to the increased speckle apparent in the original images. The detection of the shadows was not affected by the choice of parameters, which also suggests that the technique may be converging to a local minimum. The original implementation of the MRF for the sidescan data sacrificed convergence accuracy for speed, since the shadows in sidescan tended to be very clear within the data.

The Cooperating Statistical Snakes is seeking to draw contours in the image around regions with similar statistical properties. The fact that the statistics of the SAS images were different from the sidescan images did not degrade the results, since this was not considered by the technique. In this case, the increased speckle did not affect the results, in that the statistics of the shadow with speckle was still different from the seabed with speckle. This clearly shows the importance of the CSS as an integral part of the three stage process, since even when the initial MRF segmentation was not ideal the CSS enables the recovery of the correct highlight/shadow pair ready for classification.

3.3 Current trends

The improved resolution of SAS and very high resolution sidescan, particularly of the target echo, provides scope for classification based on the highlight of the target. The majority of classification systems using sidescan tend to rely on the shadow information, whereas it is proposed that exploiting the improved highlight resolution could improve the classification accuracy. It is also clear that the method proposed here for shadow extraction will also see improvements in detection and classification rates when used on SAS imagery. This has been demonstrated recently by various groups using template matching techniques for classification [Myers 2009].

The flexibility of multi-view fusion architectures can also be exploited for the classification of SAS images, since SAS also provides scope for multi-view images from the one sensor. This can be achieved by using SAS coherent beamforming to form both broadside and squint images of the same target using sub-sections of the synthetic aperture, enabling different views of the same target to be obtained. The Dempster-Shafer fusion architecture presented in[10] would permit the combination of the classification results from the sub-apertures to improve further the probability of detection and reduce false alarm rate

4 Simulation and augmented reality

Model-based methods for target detection and classification rely on the accurate modelling of the shadows from the targets. This procedure must be performed for every type of target and limits the types of objects that can be classified to those that have been previously modelled.

If a large amount of target examples are available, supervised classification methods can offer an alternative practical solution. To overcome the limited availability of real target images, synthetic ones can be generated through simulation [12]. The features and characteristics of man-made objects are well known and lead to accurate simulation of synthetic target models. Simulating Seabed realistically is more challenging.

4.1 Simulation Framework

There is an existing body of research into sonar simulation[16,17] The simulators are generally based on ray tracing techniques[18] or on a solution to the full wave equation[19]. SAS simulation takes into account the SAS processing and is, in general, highly complex[17]. Critically, in all cases, the algorithms are extremely slow (one hour to several days to compute a synthetic sidescan image with a desktop computer). When high frequencies are used, the path of the acoustic waves can be approximated by straight lines. In this case, classical ray-tracing techniques combined with a careful and detailed modelling of the energy-based sonar equation can be used. The results obtained are very similar to those obtained using more complex propagation models. Yet they are much faster and produce very realistic images. This idea was used in [16]. The simulator first generates a realistic synthetic 3D environment. The 3D environment is divided into three layers: a partition layer which assigns a seabed type to each area, an elevation profile corresponding to the general variation of the seabed, and a 3D texture that models each seabed structure. The simulator can also take into account various compositions of the seabed in terms of scattering strengths. The boundaries between each seabed type are also modelled using fractals. Objects of different shapes and different materials can be inserted into the environment. For MCM algorithms, several types of mines have been modeled such as the Manta (truncated cone shape), Rockan and cylindrical mines. The sonar images are produced from this 3D environment, taking into account a particular trajectory of the sensor (mounted on a vessel or an autonomous platforms). The seabed reflectivity is computed thanks to state-of-the-art models developed by APL-UW in the High-Frequency Ocean Environmental Acoustic Models Handbook[20] and the reflectivity of the targets is based on a Lambertian model. A pseudo ray-tracing algorithm is performed and the sonar equation is solved for each insonified area giving the backscattered energy. Note that the shadows are automatically taken into account thanks to the pseudo ray-tracing algorithm. An example of the resulting sidescan images is displayed in Figure 6. The processing time required to compute a sonar image of 50 m by 50 m using a 2 GHz Intel Core 2 Duo with 2 GB of memory is approximately 7 seconds.

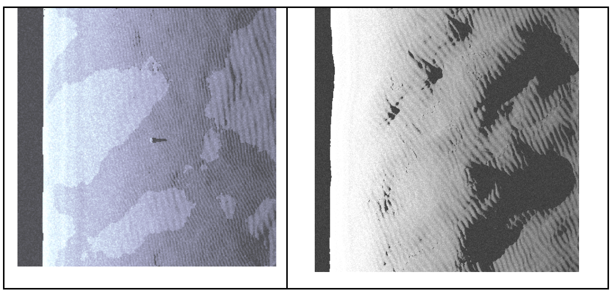

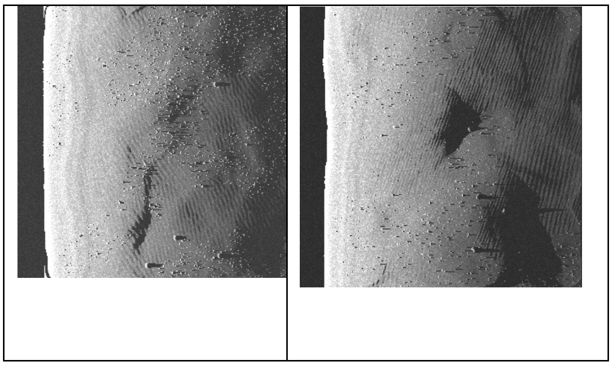

Figure 6: Examples of simulated target and texture for Mine Detection and classification missions. The simulated image contains a number of targets and 2 seabed types and two seabed textures.

4.2 Augmented Reality

However, modelling the natural seafloor is sometimes difficult. System noise, environmental inhomogeneities and image artefacts affecting sonar images in real operational conditions are also difficult to model accurately.

A compromise between using real and synthetic data can be found in the Augmented Reality (AR) simulation [13], where synthetic target models are embedded on a real image of the seafloor. A computer model of the seafloor is constructed from the sidescan image by an inversion process [14], which determines the parameters that characterize the observed scene. Then the computer model for the seafloor and that of the target are combined and rendered to obtain a new AR image that realistically integrates the synthetic target within the observed scene. This way, training images for a future mission can be generated from previous sidescan imagery of appropriate types of seabed and the computer models of the targets to be expected.

The construction of the AR training database starts by selecting appropriate sidescan sonar images and 3D computer models of target geometry. The sidescan images should be representative of the type or types of seabed to be expected in the test dataset or final mission, and ideally should have been acquired by the same model of sensor that will acquire the test data. The computer models for the targets should approximate the expected types of targets as accurately as possible. With the computer models for the images and the targets, a large number of simulated AR samples can be generated (along with their associated ground-truth) and stored in the training database.

4.2.1 Sonar Inversion

In order to generate a 3D computer model of an observed scene, it is necessary to analyze the sidescan image and try to determine what particular characteristics and properties of the seafloor and the observing sensor resulted in the formation of this image. We assume these characteristics to be represented by a set of 3 parameters per image pixel: seabed altitude Z of the point, reflectivity of the seafloor R at the point, and intensity Φ of the illuminating acoustic pulse at the point. The sonar inversion process is the means by which we are able to reconstruct these sets of parameters for a given sidescan image. A detailed explanation of this procedure can be found in [14].

In order to perform the inversion, a model for the sidescan image formation process is required. We have chosen the classical Lambertian diffuse illumination model which assumes that the observed intensity at a surface point depends only on the incidence angle to the source. Using this approach the intensity in the image can be related to the scene parameters with a forward model. The inverse problem, that of obtaining the scene parameters from a given real sidescan image, is much more complex and requires the utilization of statistical optimization techniques.

4.2.2 Generation of Augmented Reality Images

Once the height map, reflectivity and beam pattern maps from a sidescan image have been estimated, it is possible to realistically introduce simulated mines by locally modifying these maps according to the height and reflectivity that compose the synthetic model of the target (Figure 6) in order to obtain two new elevation and reflectivity maps.

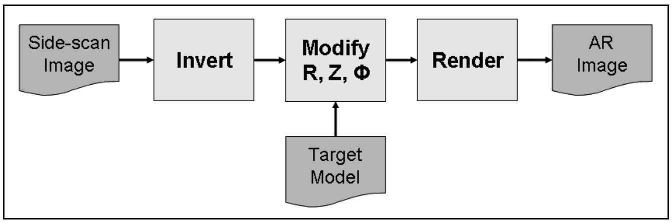

Figure 7: Augmented Reality system.

After calculating the new height map the beam-pattern map Φ has to be recomputed in order to account for the changes in elevation, since Φ(x, y) is the projection of the sonar beam-profile on the seafloor. Once the modified Z’, R’ and Φ’ maps are obtained, the Augmented Reality image can be rendered. Unlike other simulators which paste a simulated mine on top of an existing image, this approach enables the modelling of the interactions between the topography of the seabed and the mine. For instance, if a mine is placed behind a 3D structure it should not be visible. The length of the projected shadow should also depend on the local elevation of the mine.

4.3 Simulated Training Set Generation

Using the Simulation and Augmented Reality processes described in the previous section, a large number of training samples can easily be generated. 3D target models are scattered over the scene and the final simulated image is rendered. From this image, positive and negative training examples can be extracted. A ground-truth file is then generated for each image specifying the presence or absence of target, its type if present, its geo-location in the source image, etc. If an independent system to classify the seabed type is also available then the type of local seabed can also be indicated in the ground-truth file.

Since all the parameters involved in the generation of the training samples are controlled, training databases can be tailored to each particular theatre of operation. The statistical composition of the databases can also be controlled, specifying the relative quantities of targets and seafloor types as desired. Typical databases will contain several thousand samples.

Examples of positive and negative training snippets for a Marine Sonics system are presented in figure 7. The left hand columns illustrate negative samples with no targets and the right hand columns show positive samples with cylinders, truncated cones and trapezoidal targets. The sidescan image resolution is 0.058m across-track by 0.12m along-track, which results in a snippet size of 44 by 17 pixels.

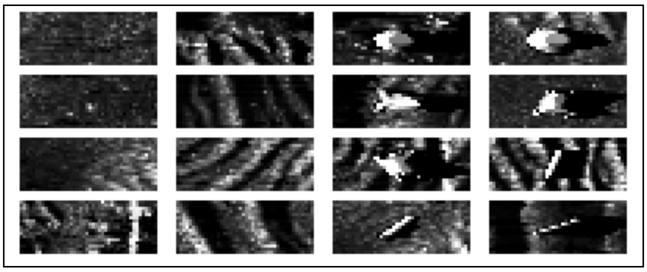

Figure 8: Augmented reality database snippets for a Marine Sonics sidescan sonar.

4.4 Detection and Classification

4.4.1 Classical classification approach

A general data classifier typically works on numerical feature vectors, which are computed from the image samples by application of a feature extractor. In a supervised classification system, a classifier is trained to discriminate between different object classes by presenting it with a vast set of examples. Application of the feature extractor to the training AR database entries will result in a large set of feature vectors and corresponding ground-truthed classes. The goal of the training procedure is to make the classifier estimate the best possible mapping between the feature vectors and their corresponding classes. After training, it is expected that the classifier will be able to generalise, upon presentation of previously unseen samples.

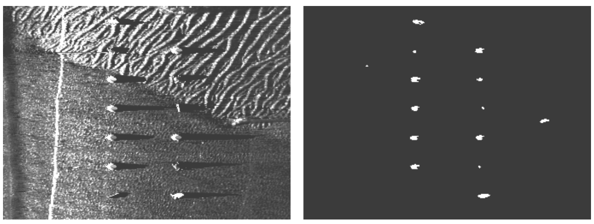

Figure 9: (a) input AR image (b) Results of detection

A range of different extractors have been examined including central filters, bi-orthogonal wavelets, thresholds, variances, templates and histogram based features. An example of the type of results obtained with the central filters is shown in Figure 8, where target detection has been performed on an augmented reality image. Thirteen objects are present in the AR image (2 type A, 6 type B, 5 type C), and the training database used contained only positive samples of targets of types B and C. The results of the detection show 100% detection of the B and C targets and 3 false alarms (a type A object, a rock and a false positive on the surface return).

An example of application of the same technique to a collage of real imagery is shown in Figure 9, where the input sidescan image contains 5 objects (1 type A, 3 type B and a non-target). Results of detection are 100% on the A and B type targets, and the non-target object produces a false alarm. The system was trained on an AR database containing A, B and C type synthetic targets on flat seabed only.

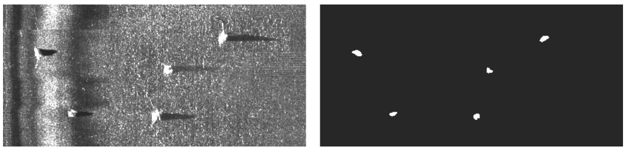

Figure 10: (a) input image (b) detection results

4.4.2 Cascade classifiers for fast detection

Introduction

Recently Haar-boosted cascade framework was f introduced by Viola and Jones [21] fir face detection and extended later in several publications such as [22]. Since then it has attracted much attention because of the tremendous speed and high detection rate it offers. This framework has three main ideas. The first idea is a new image representation called the *integral image*, which allows computing Haar features, used in this framework, very quickly. The second idea is an efficient variant of *AdaBoost*, which also acts as a feature selection mechanism. Finally and most importantly [21] introduces interestingly a simple combining classifier model referred to as the *cascade*, which speeds up the detection by rejecting most background images in the very early stages of the cascade and focus the main computation only on object like patches.

Given the fact that within any single image an overwhelming majority of sub-windows are negative (non-target), an approach is needed to rapidly determine where in an image an object might occur. The structure of the cascade reflects such a phenomenon by rejecting as many negatives as possible at the earliest stage possible. The overall form of the cascade is that of a degenerate decision tree, where at each stage a classifier is trained to detect almost all objects of interest while rejecting a certain fraction of the non-object patterns. Figure 11 shows a schematic depiction of the detection cascade. An input patch is classified as a target only if it passes the tests in all stages. Much like decision trees, subsequent classifiers are trained using those examples which pass through all the previous stages. Thus, more difficult tasks are faced by classifiers appearing at later stages.

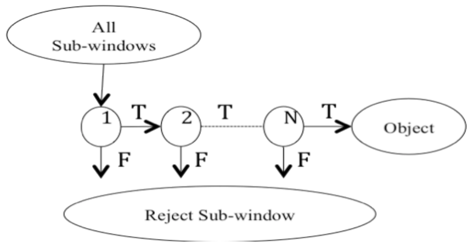

Figure 11. Schematic depiction of the detection cascade.

Stages of the cascade investigated in this paper are constructed by training classifiers using AdaBoost. The key insight is that smaller and therefore more efficient AdaBoost classifiers can be constructed to detect almost all positive examples (e.g. 99%) while rejecting plenty of the negatives (e.g. 50%). AdaBoost algorithm is not specially designed to achieve high detection rates at the expense of large false positive rates. However, this goal can be achieved by adjusting the strong classifier threshold. It is an open argument whether adjusting the threshold in this way preserves the training and generalization guarantees provided by AdaBoost. Cascade detectors have demonstrated impressive detection speed and high detection rates. In this paper, we use the cascade structure, in order to ensure high speed especially being restricted by the limited processing power of an AUV (Autonomous Underwater Vehicle).

Results:

Results presented here have been obtained using both the simulator and the Augmented reality framework presented in the previous section. In each case, several hundred simulated targets and clutter examples where used for training and testing. The Augmented reality framework used 452 images from a real mission including flat, rippled and complex terrains.

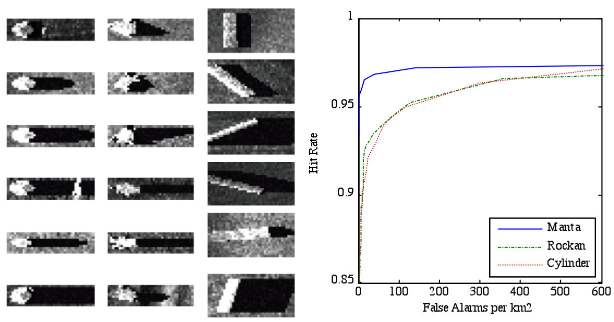

Figure 12. Snapshots of the three objects (from left to right: Manta, Rockan, and Cylinder) at different orientations, backgrounds, and ranges. ROC curve of classification results on augmented reality framework. The FA rate is stated in false alarms per square kilometre. At image level a 100 false alarms per square kilometre represents at PFA of 2.68 10^{-6}.

Similar results where obtained using the simulated data. An example of detection in a complex image is given in Figure 13 below.

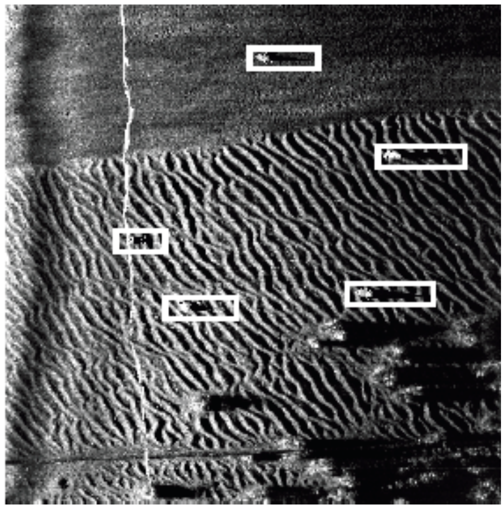

Figure 13. Detection of Manta Targets in a complex environment.

4.6 Adaptive planning for target identification

A new and important aspect of Mine detection and identification is the ability to adapt the mission on the fly to improve classification results or guarantee minimum detection rate. The first aspect can be achieve using multiview classification[23]. The second one requires online mission planning coupled with real time seabed classification. If the latter can be achieved, performances of the detection and classification algorithms (obtained in simulation using the augmented reality framework) can be used to predict the likely detection rate. The mission can then be adapted to guarantee a specific detection performance. The algorithm is akin to a travelling salesman problem and has been described in [24]. An example of real mission adaptation is given in figure 14.

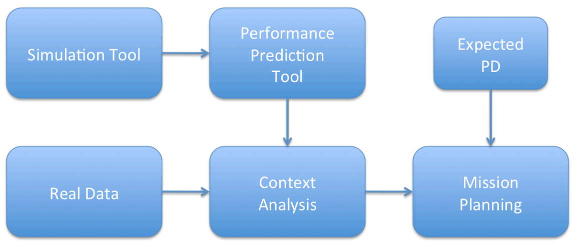

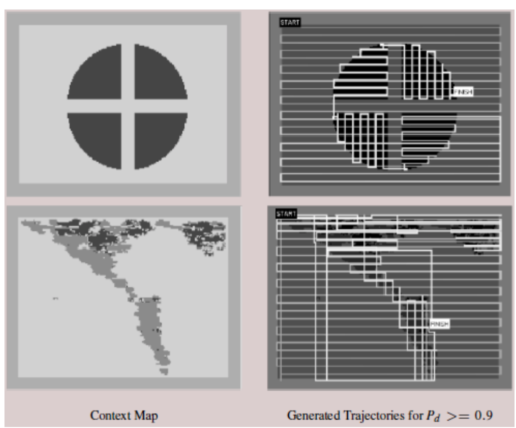

Figure 14. Principle of the performance prediction and adaptive mission planning for automated MCM missions.

5 Conclusions

This paper has reviewed model based and machine learning based existing approaches for mine detection and classification and proposed new ideas to solve the issues around accurate detection and classification in emerging SAS sonar imagery. The first approach illustrated a three stage model based system for detection and classification of objects in sidescan imagery and illustrated how the system is directly applicable to SAS. The improved resolution of the SAS highlight (and higher resolution sidescan with improved highlight resolution) also suggests the extension of the model based classification to consider the highlight as well as shadow. Since the simple line of sight model used to simulate the shadows in the sidescan classification system may prove to be inadequate for the SAS imagery anyway, a more complex model may need to be considered.

The second approach employed an augmented reality simulator to produce large databases of targets specific to the sonar being utilised and the seabed type of interest. Initial results of classification on this synthetic data were illustrated for sidescan imagery. The technique as stands can also be used directly to produce synthetic images of very high resolution sidescan and SAS.

New emerging techniques inherited from the computer vision community have been briefly presented and evaluated and have shown promises to enable reliable and fast detection and classification in real time in SAS imagery.

However, one issue raised by both systems is what resolution is needed for accurate detection and classification and will improved resolution increase significantly the success of CAD/CAC algorithms. This problem is currently under study in our group.

7 References

[1] T. Aridgides, M. Fernandez and G. Dobeck, “Adaptive 3 Dimensional range-crossrange-frequency filter processing string for sea mine classification in sidescan sonar imagery” Proc SPIE, 3079, 111-122, 1997

[2] B.R. Calder, L.M. Linnett and D.R. Carmichael, “Spatial stochastic models for seabed object detection” Proc SPIE, 3079, 1997

[3] C.M. Ciany and J.Huang, “Computer aided detection/computer aided classification and data fusion algorithms for automated detection and classification of underwater mines” Proc. MTS/IEEE Oceans Conf. And Exhibition, 1:277-284,2000

[4] S.Reed, Y.Petillot, J. Bell, “An Unsupervised Approach to the Detection and Extraction of Mine Features in Sidescan Sonar”, IEEE J. Oceanic Engineering 28(1), 90-105, Jan 2003

[6] G.J. Dobeck, J.C. Hyland and L. Smedley, “Automated detection/classification of sea mines in sonar imagery”, Proc SPIE, 3079, pp. 90-110, 1997

[7] E. Dura, J. Bell and D. Lane, “Superellipse fitting for the classification of mine-like shapes in side-scan sonar imagery”, IEEE/MTS Oceans 2002, pp. 23-28, 2002

[8] J.A. Fawcett, “Image based classification of sidescan sonar detections”, presented at CAD/CAC Conf. Halifax, Canada, Nov 2001

[10] S.Reed, Y.Petillot, J. Bell, “Automated approach to the classification of mine-like objects in sidescan sonar using highlight and shadow information”, IEE Proceedings – Radar, Sonar and Navigation, 151(1), pp. 48-56, Feb 2004

[11] G.J. Dobeck, “Algorithm Fusion for automated sea-mine detection and classification”, Oceans 2001, 1, 130-134

[12] J. Bell, M. Lianantonakis, “Analysis of Target Scattering using a Finite Difference Time Domain Model”, Proc IOA Vol 27, Pt 1, 2005

[13] E. Coiras, Y. Petillot and D. Lane, Multi-Resolution 3D Reconstruction from Side-Scan Sonar Images, IEEE Transactions on Image Processing, Vol. 16, No 2, pp 382-390, January 2007.

[14] E Coiras, Y Petillot, D M Lane, An Expectation-Maximization Framework for the Estimation of Bathymetry from Side-scan Sonar Images, Oceans 2005, Brest, France, Vol. 1, pp 261-264, June 2005

[15] Y. Pailhas, Y. Petillot, C. Capus and K. Brown,
Real-time Sidescan Simulator and Applications
IEEE Oceans 2009 Europe Conferences, Bremen

[16] J. Bell, “A model for the simulation of sidescan sonar,” Ph.D. dissertation, Heriot-Watt University, August 1995.

[17] A. J. Hunter, M. P. Hayes, and P. T. Gough, “Simulation of multiplereceiver, broad- band interferometric sas imagery,” in IEEE OCEANS Conf. Proc., 2003.

[18] J. Bell, Application of optical ray tracing techniques to the simulation of sonar images, Optical Engineering, vol. 36(6), pp. 1806–1813, 1997.

[19] G. Elston and J. Bell, Pseudospectral time-domain modeling of nonrayleigh reverberation: synthesis and statistical analysis of a sidescan sonar image of sand ripples, Oceanic Engineering, IEEE Journal of, vol. 29(2), pp. 317–29, 2004.

[20] A. P. L. at the University of Washington, High-Frequency Ocean Environmental Acoustic Models Handbook. Technical Report APLUW TR 9407, October 1994.

[21] P. Viola, M. Jones, "Robust real-time object detection," In Workshop on Statistical and Computational Theories of Vision, 2001.

[22] R. Lienhart, J. Maydt, "An Extended Set of Haar-like Features for Rapid Object Detection," IEEE ICIP 2002, Vol. 1, pp.

[23] S. Reed, Y. Petillot and J. Bell, Automated approach to classification of mine-like objects in sidescan sonar using highlight and shadow information, IEE Proceeding Radar, Sonar and Navigation, Vol. 151, pp 48-56, Feb 2004

[24] Automated Mission Planning for Mine Counter Measure
Operations, MSc Dissertation, Heriot-Watt University, 2006.